

A non-Gaussian landscape

Sami Nurmi ^{a*}, **Christian T. Byrnes** ^{b†}, **Gianmassimo Tasinato** ^{c‡}

^a *Department of Physics and Helsinki Institute of Physics, University of Helsinki, P.O. Box 64, FIN-00014 University of Helsinki, Finland*

^b *Astronomy Centre, University of Sussex, Brighton, BN1 9QH, UK*

^c *Institute of Cosmology & Gravitation, University of Portsmouth, PO1 3FX, UK*

ABSTRACT: Primordial perturbations with wavelengths greater than the observable universe shift the effective background fields in our observable patch from their global averages over the inflating space. This leads to a landscape picture where the properties of our observable patch depend on its location and may significantly differ from the expectation values predicted by the underlying fundamental inflationary model. We show that if multiple fields are present during inflation, this may happen even if our horizon exit would be preceded by only a few e-foldings of inflation. Non-Gaussian statistics are especially affected: for example models of local non-Gaussianity predicting $|f_{\text{NL}}^0| \gg 10$ over the entire inflating volume can have a probability up to a few tens of percent to generate a non-detectable bispectrum in our observable patch $|f_{\text{NL}}^{\text{obs}}| \lesssim 10$. In this work we establish systematic connections between the observable local properties of primordial perturbations and the global properties of the inflating space which reflect the underlying high energy physics. We study in detail the implications of both a detection and non-detection of primordial non-Gaussianity by Planck, and discover novel ways of characterising the naturalness of different observational configurations.

*sami.nurmi@helsinki.fi

†ctb22@sussex.ac.uk

‡gianmassimo.tasinato@port.ac.uk

Contents

1. Introduction	1
2. The curvature perturbation	2
2.1 Long wavelength modes	3
3. Probability distributions of local observables	5
3.1 Spectrum, bispectrum and trispectrum	5
3.2 How large are the variances?	7
4. Implications on inflationary physics	9
4.1 Small primordial non-Gaussianity	9
4.2 Large primordial non-Gaussianity	11
4.3 Non-Gaussian signatures and fine-tuning	13
5. Extension and applications of our results	15
5.1 Variance of the power spectrum in multi-source scenarios	15
5.2 What will we observe if the single-source equality is broken by loops?	16
6. Conclusions	17

1. Introduction

Inflation is the leading scenario explaining the generation of primordial perturbations. The imminent release of Planck data will provide crucial new information of the non-Gaussian statistics of primordial perturbations. This will help to efficiently discriminate between different realisations of inflation, potentially ruling out whole classes of models. Future Large Scale Structure surveys like Euclid will further improve our knowledge of the statistics of primordial perturbations opening striking new insights to the high energy physics behind inflation.

The observable primordial perturbations probe physics during the last $N_{\text{obs.}} \sim 60$ e-foldings of inflation after the horizon exit of the largest observable modes. Inflation may however have lasted much longer, so that the observable part of the universe would constitute only a fraction of the entire inflating patch. Long-wavelength perturbations generated before the horizon exit of largest observable scales average to constants over our observable patch, effectively shifting the local background field values. In adiabatic single-field models it is well known that the long-wavelength contributions amount to simply shifting the local time coordinate [1]. The situation is different if more than one light

dynamical scalar is present during inflation, as in many models generating detectable non-Gaussianity. In this case the evolution is non-adiabatic and the long-wavelength modes in general shift both the time coordinate and the fields parameterizing isocurvature directions. Shifts in the isocurvature directions correspond to non-trivial changes of initial conditions which may significantly affect the observational signatures and especially the non-Gaussian statistics, irrespective of whether the isocurvature perturbations persist until today.

The long-wavelength contributions are different in different parts of the inflating region which generates variances in the physical properties of patches smaller than the entire inflating region. This leads to a landscape picture where the statistics of perturbations within a horizon patch depend on the location of the patch itself [2], as previously discussed in the curvaton scenario [3, 4]. The observable perturbations can of course be described by an effective model covering only the last N_{obs} e-foldings of inflation in our horizon patch. The background field values in the effective description are modulated by a random long-wavelength contribution specific to our location in the entire inflating patch. In the presence of isocurvature directions the effective model can be non-trivially related to the underlying fundamental inflationary model which covers the entire inflationary epoch $N_{\text{tot.}}$. Given a fundamental model with $N_{\text{tot.}} > N_{\text{obs.}}$ it is not possible to make firm predictions for the observable signatures in our horizon patch but one is led to consider probabilities of different signatures. It turns out that especially in non-Gaussian models the differences between the entire inflating patch, and of a random patch the size of our observable patch, can be significant. This is the case even if the horizon exit of the largest observable modes would be preceded by just a few e-foldings of inflation.

Since the fundamental model of inflation should be confronted with theories of high-energy physics, it is of crucial importance to develop a solid understanding of its relation to the effective description of the last N_{obs} e-foldings, which in turn can be directly confronted with the observations made in our horizon patch. In this work we will make systematic progress towards this goal. We will establish novel relations between the observable signatures and the form of the underlying inflationary physics. Our model independent approach opens up interesting new possibilities to address the naturalness of different non-Gaussian signatures. By making use of these findings, we will establish new connections between large and small non-Gaussianity and the structure of inflationary physics.

2. The curvature perturbation

We concentrate on the class of generic single source models where the dominant contribution to curvature perturbation is due to a single scalar field, known as single-source inflation [5]. This field can be an isocurvature degree of freedom during inflation, e.g. the curvaton scenario [6, 7] or modulated reheating [8, 9]. Such models can easily generate observable non-Gaussianity. In the presence of isocurvature directions, the long-wavelength fluctuations can not be removed by merely shifting the time coordinate like in the adiabatic single field case [1]. Consequently, the long-wavelength modes can have interesting observational consequences.

We assume the non-Gaussianity is generated on superhorizon scales and neglect all contributions from subhorizon modes. While some non-Gaussianity is in general also produced by subhorizon physics, these contributions are slow roll suppressed in models with canonical kinetic terms. In this class of models the leading contribution to observable non-Gaussianities is therefore generated by superhorizon physics.

Neglecting the subleading subhorizon contributions, the curvature perturbation ζ can be expressed in the local form

$$\zeta(\mathbf{x}) = \zeta_G(\mathbf{x}) + \frac{3}{5} f_{\text{NL}}^0 (\zeta_G^2(\mathbf{x}) - \langle \zeta_G^2 \rangle) + \left(\frac{3}{5}\right)^2 g_{\text{NL}}^0 \zeta_G^3(\mathbf{x}) + \left(\frac{3}{5}\right)^3 h_{\text{NL}}^0 (\zeta_G^4(\mathbf{x}) - \langle \zeta_G^4 \rangle) + \dots \quad (2.1)$$

Here ζ_G is a Gaussian field and the tree-level coefficients f_{NL}^0 , g_{NL}^0 etc. are constants. We are neglecting a possible scale dependence of the non-linearity parameters, as discussed for example in [10].

The local Ansatz amounts to assuming that ζ is an analytic function of a single Gaussian inhomogeneous field. To make this manifest, we can equivalently rewrite (2.1) as

$$\zeta(\mathbf{x}) = \sum_{n=1}^{\infty} \frac{N^{(n)}(\sigma_0)}{n!} \delta\sigma^n(\mathbf{x}) , \quad (2.2)$$

where σ_0 denotes a classical homogeneous solution of equations of motion (and we understand that we remove from the even powers in the previous formula the averages over the entire space, to make the average of ζ over all space vanishing). This corresponds to the familiar δN expression [11] if $\delta\sigma(\mathbf{x}) = \zeta_G(\mathbf{x})/N'(\sigma_0)$ are chosen to represent fluctuations on a spatially flat hypersurface soon after the horizon exit. $N(\sigma)$ then measures the number of e-foldings from that hypersurface to a uniform energy hypersurface at which ζ is frozen to a constant value (which must exist provided that all isocurvature perturbations decay).

To set the notation: the spectrum, bispectrum and trispectrum are parameterized by

$$\begin{aligned} \langle \zeta_{\mathbf{k}_1} \zeta_{\mathbf{k}_2} \rangle &= (2\pi)^3 \delta(\sum \mathbf{k}_i) P_0(k_1) , \\ \langle \zeta_{\mathbf{k}_1} \zeta_{\mathbf{k}_2} \zeta_{\mathbf{k}_3} \rangle &= (2\pi)^3 \delta(\sum \mathbf{k}_i) (f_{\text{NL}}^0 P_0(k_1) P_0(k_2) + \text{perms.}) , \\ \langle \zeta_{\mathbf{k}_1} \zeta_{\mathbf{k}_2} \zeta_{\mathbf{k}_3} \zeta_{\mathbf{k}_4} \rangle &= (2\pi)^3 \delta(\sum \mathbf{k}_i) (g_{\text{NL}}^0 P_0(k_1) P_0(k_2) P_0(k_3) + \\ &\quad + \tau_{\text{NL}}^0 P_0(k_1) P_0(k_2) P_0(k_3) P_0(|\mathbf{k}_1 + \mathbf{k}_2|) + \text{perms.}) . \end{aligned} \quad (2.3)$$

Since we are considering single source scenarios, the tree-level parameters f_{NL}^0 and τ_{NL}^0 are related by $\tau_{\text{NL}}^0 = (6/5)^2 (f_{\text{NL}}^0)^2$ [12, 13].

2.1 Long wavelength modes

Let us consider the impact of long-wavelength fluctuations of the field σ in the expression for the curvature perturbation (2.2). We denote by σ_0 the classical homogeneous solution which corresponds to the spatial average of $\sigma(\mathbf{x})$ over the entire inflating patch. Fluctuations

around the global background can be divided into long and short wavelength components with respect to the horizon scale of the observable universe $k_{\text{obs.}} = a_{\text{obs.}} H_{\text{obs.}}$.

$$\delta\sigma(\mathbf{x}) = \int_{q>k_{\text{obs.}}} \frac{d\mathbf{q}}{(2\pi)^3} e^{i\mathbf{q}\cdot\mathbf{x}} \delta\sigma(\mathbf{q}) + \int_{q<k_{\text{obs.}}} \frac{d\mathbf{q}}{(2\pi)^3} e^{i\mathbf{q}\cdot\mathbf{x}} \delta\sigma(\mathbf{q}) \equiv \delta\sigma_{\text{s}}(\mathbf{x}) + \delta\sigma_{\text{L}}(\mathbf{x}) . \quad (2.4)$$

To first order in perturbations the long- and short-wavelength modes are uncorrelated, $\langle \delta\sigma_{\text{L}}(\mathbf{k}) \delta\sigma_{\text{s}}(\mathbf{k}') \rangle = 0$, and they both have vanishing ensemble averages, $\langle \delta\sigma_{\text{L}} \rangle = \langle \delta\sigma_{\text{s}} \rangle = 0$. The ensemble averages are assumed to coincide with the spatial averages computed over the entire inflating patch, hence $\langle \sigma(\mathbf{x}) \rangle = \sigma_0$.

Spatial averages computed over regions smaller than the inflating patch in general differ from the ensemble averages. This is due to the long-wavelength modes. For example, the average of $\delta\sigma_{\text{L}}$ over a spherical patch with radius $k_{\text{obs.}}^{-1}$ and origin at \mathbf{x}_0 reads

$$\begin{aligned} \langle \delta\sigma_{\text{L}}(\mathbf{x}) \rangle_{\text{obs.}, \mathbf{x}_0} &\equiv \frac{1}{V_{\text{obs.}}} \int d\mathbf{x} \theta(k_{\text{obs.}}^{-1} - |\mathbf{x} - \mathbf{x}_0|) \delta\sigma_{\text{L}}(\mathbf{x}) \\ &= \frac{1}{V_{\text{obs.}}} \int \frac{d\mathbf{q}}{(2\pi)^3} \theta(k_{\text{obs.}} - q) \delta\sigma(\mathbf{q}) e^{i\mathbf{q}\cdot\mathbf{x}_0} V_{\text{obs.}} \left(1 + \mathcal{O}\left(\frac{q^2}{k_{\text{obs.}}^2}\right) \right) \\ &\simeq \delta\sigma_{\text{L}}(\mathbf{x}_0) . \end{aligned} \quad (2.5)$$

In order to pass from second to last line, we have assumed a scale invariant form for the mode functions, $\delta\sigma(q) \propto q^{-3/2}$.

In a similar way one finds $\langle \delta\sigma_{\text{L}}^n(\mathbf{x}) \rangle_{\text{obs.}, \mathbf{x}_0} \simeq \delta\sigma_{\text{L}}^n(\mathbf{x}_0)$, so that the curvature perturbation (2.1) in a patch the size of our observable universe $k_{\text{obs.}}^{-1}$ can be written as

$$\zeta_{\text{obs.}}(\mathbf{k}) \simeq \sum_{n=1}^{\infty} \frac{N^{(n)}(\sigma_0 + \delta\sigma_{\text{L}}(\mathbf{x}_0))}{n!} (\delta\sigma_{\text{s}}(\mathbf{k}))^n . \quad (2.6)$$

Here $\delta\sigma_{\text{L}}(\mathbf{x}_0)$ is a constant in $\langle \dots \rangle_{\text{obs.}, \mathbf{x}_0}$ (but not in $\langle \dots \rangle$ since it depends on the position \mathbf{x}_0). We have adopted a notation where $X_{\text{obs.}}$ denotes a quantity X evaluated in a patch of the size of our observable universe.

The results depend on the location \mathbf{x}_0 of the patch as the contribution of long-wavelength modes is different in different regions of the inflating space. This position dependence limits our ability to make precise predictions for observables in our horizon patch [14] if $N_{\text{tot.}} > N_{\text{obs.}}$. Instead of assuming that we would occupy a “typical” location as in [14] we follow a top down approach and systematically relate the probabilities for different observational configurations in our patch to the form of the underlying fundamental inflationary physics. Given an inflationary model with initial conditions set at the beginning of inflation, we can make precise predictions only for spatial averages over the entire inflating patch. These can significantly differ from the averages in our horizon patch due to the unknown long-wavelength contributions. However, given a model we can unambiguously compute the probabilities for different observational configurations in our horizon patch and thus work out the possible observational imprints of the model. Going in the opposite direction, we can also convert the observational information into constraints on the fundamental high-energy physics controlling the evolution of the entire inflating patch.

In this work we will systematically explore the consequences of the long-wavelength modulations. We will establish novel connections between the effective inflationary physics describing our observable patch, and the fundamental inflationary physics which dictates the statistics of perturbations over all of the inflating space and directly reflects the underlying high-energy physics.

3. Probability distributions of local observables

If inflation lasted longer than $N_{\text{obs.}} \sim 60$ e-foldings, our observable universe constitutes an exponentially small fraction of the entire inflating space. Patches of our horizon size $(a_{\text{obs.}} H_{\text{obs.}})^{-1}$ located in different places of the universe can then have different physical properties. This is a consequence of the long-wavelength fluctuations which generate a random modulation in the local expansion history. The modulation is proportional to the number of e-foldings before the horizon exit of our observable region

$$N_{\text{in.}} \equiv \ln \frac{a_{\text{obs.}} H_{\text{obs.}}}{a_0 H_0} , \quad (3.1)$$

where t_0 stands for the beginning of inflation. The longer the duration of inflation, the more the unknown long-wavelength contributions limit our ability to directly probe the underlying high energy physics reflected in the statistics of inflationary perturbations over the entire inflating space.

3.1 Spectrum, bispectrum and trispectrum

We assume that the fluctuations at horizon crossing $\delta\sigma = \zeta_{\text{G}}/N'$ in (2.2) are Gaussian so that all correlators can be expressed in terms of the two-point function

$$\langle \delta\sigma(\mathbf{k}) \delta\sigma(\mathbf{k}') \rangle = (2\pi)^3 \delta(\mathbf{k} + \mathbf{k}') P_{\delta\sigma}(k) = (2\pi)^3 \delta(\mathbf{k} + \mathbf{k}') \frac{2\pi^2}{k^3} \mathcal{P}_{\delta\sigma} . \quad (3.2)$$

For the canonical models of inflation we are concentrating on, $\mathcal{P}_{\delta\sigma} \simeq (H/2\pi)^2$ and the dependence of $H(t, \sigma)$ on the field σ is slow roll suppressed. In the following we will neglect this dependence so that the two point function of $\delta\sigma$ computed over an arbitrary subregion of the inflating patch is given by the ensemble average (3.2). In what follows we will also ignore the slow roll suppressed scale dependence of $\mathcal{P}_{\delta\sigma}$.

Using (2.6), the spectrum of curvature perturbations in a patch the size of our observable universe is given by

$$\mathcal{P}_{\text{obs.}} = \mathcal{P}_0 \left(1 + \frac{12}{5} f_{\text{NL}}^0 N'(\sigma_0) \delta\sigma_{\text{L}}(\mathbf{x}_0) \right) , \quad (3.3)$$

to first order in the long-wavelength field. $\mathcal{P}_0 = N'^2(\sigma_0) \mathcal{P}_{\delta\sigma}$ and $f_{\text{NL}}^0 = 5N''(\sigma_0)/6N'^2(\sigma_0)$ denote the ensemble expectation values of the spectrum and the bispectrum amplitude, which coincide with spatial averages over the entire inflating patch.

Hence, the spectrum $\mathcal{P}_{\text{obs.}}$ of fluctuations in a horizon size patch depends on the location \mathbf{x}_0 of the patch through the Gaussian field $\delta\sigma_{\text{L}}(\mathbf{x}_0)$. This gives rise to a landscape

picture where the amplitude of curvature perturbations measurable locally on patches of size $(a_{\text{obs.}} H_{\text{obs.}})^{-1}$ fluctuates around the global average \mathcal{P}_0 according to a Gaussian probability distribution

$$P(\mathcal{P}_{\text{obs.}}) = (2\pi\sigma_{\mathcal{P}}^2)^{-1/2} \exp\left(-\frac{(\mathcal{P}_{\text{obs.}} - \mathcal{P}_0)^2}{2\sigma_{\mathcal{P}}^2}\right). \quad (3.4)$$

Here the variance is given by

$$\sigma_{\mathcal{P}}^2 = \left(\frac{12}{5} f_{\text{NL}}^0 \mathcal{P}_0\right)^2 N'^2(\sigma_0) \langle \delta\sigma_{\text{L}}^2(\mathbf{x}_0) \rangle \simeq \left(\frac{12}{5} f_{\text{NL}}^0\right)^2 \mathcal{P}_0^3 N_{\text{in.}}. \quad (3.5)$$

In a similar way, using equation (2.6) and working to first order in $\delta\sigma_{\text{L}}$, we can calculate the probability distributions for $f_{\text{NL}}^{\text{obs.}}$, $\tau_{\text{NL}}^{\text{obs.}}$ and $g_{\text{NL}}^{\text{obs.}}$ measuring the non-Gaussian statistics in a horizon size patch. The results are given by

$$P(f_{\text{NL}}^{\text{obs.}}) = \frac{\exp\left(-\frac{(f_{\text{NL}}^{\text{obs.}} - f_{\text{NL}}^0)^2}{2\sigma_{f_{\text{NL}}}^2}\right)}{\sqrt{2\pi\sigma_{f_{\text{NL}}}^2}}, \quad \sigma_{f_{\text{NL}}}^2 = \left(\frac{9}{5} g_{\text{NL}}^0 - \frac{12}{5} (f_{\text{NL}}^0)^2\right)^2 \mathcal{P}_0 N_{\text{in.}}, \quad (3.6)$$

$$P(g_{\text{NL}}^{\text{obs.}}) = \frac{\exp\left(-\frac{(g_{\text{NL}}^{\text{obs.}} - g_{\text{NL}}^0)^2}{2\sigma_{g_{\text{NL}}}^2}\right)}{\sqrt{2\pi\sigma_{g_{\text{NL}}}^2}}, \quad \sigma_{g_{\text{NL}}}^2 = \left(\frac{12}{5} h_{\text{NL}}^0 - \frac{18}{5} g_{\text{NL}}^0 f_{\text{NL}}^0\right)^2 \mathcal{P}_0 N_{\text{in.}}, \quad (3.7)$$

where h_{NL}^0 is defined as the fourth order coefficient in the expansion of the curvature perturbation (2.1). The non-linearity parameter $\tau_{\text{NL}}^{\text{obs.}}$ in each patch is given by $\tau_{\text{NL}}^{\text{obs.}} = (6/5)^2 (f_{\text{NL}}^{\text{obs.}})^2$ at scales corresponding to the patch size. This is a result of the single source form of the curvature perturbation $\zeta_{\text{obs.}}$ (2.6). At smaller scales the relation may become violated by the loop corrections as discussed in [15].

Notice that the dependence of inflationary observables on the location of the patch is closely associated to semiclassical loop contributions to observable quantities, as we investigated in [2, 15] in collaboration with D. Wands. The difference between the curvature perturbation ζ_0 over the entire inflating patch and the curvature perturbation $\zeta_{\text{obs.}}$ in our observable patch is due to the long-wavelength modes $a_0 H_0 < k < a_{\text{obs.}} N_{\text{obs.}}$ generated before our horizon exit. Integrating over the unobservable long wavelength modes to find $\zeta_{\text{obs.}}$ (2.6) amounts to computing radiative corrections to ζ_0 at the scale $k_{\text{obs.}} = a_{\text{obs.}} H_{\text{obs.}}$. As explained in [2, 15], the radiative corrections to an n -point function of curvature perturbation consist of both the usual loop corrections, where internal momenta are integrated over, and of soft limits of higher order n -point functions where external momenta become unobservably small. The soft contributions generate variances for the n -point functions of $\zeta_{\text{obs.}}$ causing the properties of a patch the size of our observable horizon to depend on its location within the entire inflating space. It is precisely the ramifications of this effect that we are investigating in the current work.

As also explained in [2, 15], the next to leading order long-wavelength corrections to $\mathcal{P}_{\text{obs.}}$, $f_{\text{NL}}^{\text{obs.}}$, $\tau_{\text{NL}}^{\text{obs.}}$, $g_{\text{NL}}^{\text{obs.}}$ associated with higher powers of \mathcal{P}_0 are subdominant with respect to the leading order corrections as long as the bare non-linearity parameters f_{NL}^0 , g_{NL}^0 , h_{NL}^0

etc. are not extremely large. In this work we are not considering such extreme values and our first order analysis of the long-wavelength corrections is therefore justified and self consistent.

3.2 How large are the variances?

The variances generated by the long-wavelength fluctuations are uninterestingly small if there was basically no inflation before the horizon exit of the largest observable modes, $N_{\text{in.}} \lesssim \mathcal{O}(1)$, and if the ensemble expectation values of the non-Gaussian amplitudes are small, $|f_{\text{NL}}^0| \lesssim \mathcal{O}(1)$, $|g_{\text{NL}}^0| \lesssim (f_{\text{NL}}^0)^2$. The more one deviates from either of these conditions, the bigger the variances become.

The growing variances affect the comparison of inflationary models and cosmological observations in two different ways. As the variances of the theoretical predictions for the observables get bigger than the observational sensitivity, the bounds on model parameters get weakened, and projection of observational constraints on the space of model parameters may also become non-trivial. Comparing the variance $\sigma_{\mathcal{P}}$ of the spectrum $\mathcal{P}_{\text{obs.}}$, given by equation (3.5) to the $1\text{-}\sigma$ error $\Delta\mathcal{P}/\mathcal{P} \simeq 0.1$ in *WMAP* 7-years parameter fits, we find that the theoretical uncertainty dominates over the observational inaccuracy if

$$\sigma_{\mathcal{P}} > \Delta\mathcal{P} \quad \Leftrightarrow \quad \frac{|f_{\text{NL}}^0|}{50} \gtrsim \left(\frac{N_{\text{in.}}}{300} \right)^{-1/2}. \quad (3.8)$$

Here we have set $\mathcal{P}_0 = 2.44 \times 10^{-9}$. For inflationary modes featuring a few hundreds of e-foldings, $N_{\text{in.}} \gtrsim \mathcal{O}(10^2)$, the variance becomes comparable to the observational accuracy for $|f_{\text{NL}}^0| \gtrsim \mathcal{O}(10)$. This has the effect of broadening the region of parameter space compatible with observations. The growing variance increases the class of models with different super-horizon scale properties, and underlying inflationary physics, but degenerate predictions on observable scales.

The variance of the spectrum can dominate over the expectation value, $\sigma_{\mathcal{P}} \gtrsim \mathcal{P}_0$, if the inflationary model features extreme non-Gaussianities, e.g. $|f_{\text{NL}}^0| \gg 10^2$, and/or a very long period of inflation $N_{\text{in.}} \gg 10^3$. In both cases one should go beyond first order in the long-wavelength perturbations $\delta\sigma_{\text{L}}$. A more subtle issue is that the validity of the entire semiclassical approach, justifying the use of the expansion (2.2), may become questionable in the regime where fluctuations grow large: this is the regime investigated for example in [3] in the case of the curvaton scenario. In this work, we restrict ourselves to the regime of small perturbations, tractable by a first order analysis in $\delta\sigma_{\text{L}}$, where the semiclassical approach should provide an accurate description of the system. Consequently, we will not encounter situations where the variance $\sigma_{\mathcal{P}}$ would dominate over the global background \mathcal{P}_0 .

For the bispectrum the situation is different. Comparing the variances of the spectrum (3.4) and bispectrum (3.6), we obtain the relation

$$\frac{\sigma_{f_{\text{NL}}}^2}{(f_{\text{NL}}^0)^2} = \left(1 - \frac{3}{4} \frac{g_{\text{NL}}^0}{(f_{\text{NL}}^0)^2} \right) \frac{\sigma_{\mathcal{P}}^2}{\mathcal{P}_0^2}. \quad (3.9)$$

Clearly, for models with $|g_{\text{NL}}^0| \lesssim (f_{\text{NL}}^0)^2$ the relative variances are of equal magnitude. Using the expected 1- σ sensitivity of Planck, $\Delta f_{\text{NL}} = 5$ [16], we then find that the theoretical uncertainty for $f_{\text{NL}}^{\text{obs.}}$ becomes comparable or dominates over the observational accuracy, $\sigma_{f_{\text{NL}}} \gtrsim \Delta f_{\text{NL}}$, for

$$|f_{\text{NL}}^0| \gtrsim 5 \left(\frac{\sigma_{\mathcal{P}}}{\mathcal{P}_0} \right)^{-1}. \quad (3.10)$$

As we will discuss below, this can happen in the regime $\sigma_{\mathcal{P}} < \Delta \mathcal{P}$ where the theoretical variance of the spectrum is still small compared to the observational accuracy, and we may set $\mathcal{P}_{\text{obs.}} \simeq \mathcal{P}_0$ to a reasonable accuracy.

On the other hand, for models with $|g_{\text{NL}}^0| \gg (f_{\text{NL}}^0)^2$, the variance of the bispectrum can become very large even if our horizon exit was preceded by just a few e-foldings of inflation. It may even dominate over the background value, $\sigma_{f_{\text{NL}}} \gtrsim |f_{\text{NL}}^0|$, effectively screening the underlying inflationary physics which determines the global structure of the inflating space and reflects the fundamental high energy physics behind inflation. While the global average f_{NL}^0 represents the most probable value also in patches the size of our observable universe, the probability for observing a drastically different bispectrum amplitude $f_{\text{NL}}^{\text{obs.}}$ becomes significant as the variance $\sigma_{f_{\text{NL}}}$ grows large. This is illustrated in Fig. 1 for the specific example where $f_{\text{NL}}^0 = 0$ globally but the model may still result a detectable bispectrum $f_{\text{NL}}^{\text{obs.}}$ in our observable patch.

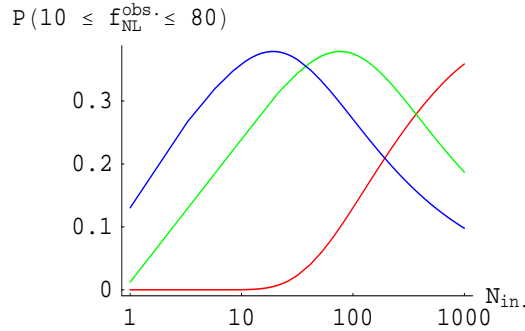


Figure 1: The probability to find $10 \leq f_{\text{NL}}^{\text{obs.}} \leq 80$ in our observable part of the universe for different values of g_{NL}^0 , assuming that the bispectrum averaged over the entire inflating patch vanishes $f_{\text{NL}}^0 = 0$. The probability is plotted against, $N_{\text{in.}}$, the number of e-foldings from the beginning of inflation up to the horizon exit of our observable patch. The three curves correspond to $g_{\text{NL}}^0 = 10^4$ (red, rightmost), $g_{\text{NL}}^0 = 5 \times 10^4$ (green, middle) and $g_{\text{NL}}^0 = 10^5$ (blue, leftmost), and we have set $\mathcal{P}_0 = 2.44 \times 10^{-9}$.

The variance of the trispectrum may also be large. As we are considering single source models, the observable $\tau_{\text{NL}}^{\text{obs.}}$ calculated using (2.6) is, at the scale $k_{\text{obs.}} = a_{\text{obs.}} H_{\text{obs.}}$ corresponding to the tree-level in the observable universe, completely determined by $f_{\text{NL}}^{\text{obs.}}$ through the relation $\tau_{\text{NL}}^{\text{obs.}} = (6/5)^2 (f_{\text{NL}}^{\text{obs.}})^2$. Its variance is then given by

$$\sigma_{\tau_{\text{NL}}}^2 = 4 \left(\frac{6}{5} \right)^4 (f_{\text{NL}}^0)^2 \sigma_{f_{\text{NL}}}^2 = 4 (\tau_{\text{NL}}^0)^2 \frac{\sigma_{f_{\text{NL}}}^2}{(f_{\text{NL}}^0)^2}. \quad (3.11)$$

It dominates over the background, $\sigma_{\tau_{\text{NL}}}^2 \gtrsim (\tau_{\text{NL}}^0)^2$, under the same conditions as $\sigma_{f_{\text{NL}}}^2 \gtrsim (f_{\text{NL}}^0)^2$. Looking at the equation (3.7), we also find that the variance of g_{NL} may become large, $\sigma_{g_{\text{NL}}}^2 \gtrsim (g_{\text{NL}}^0)^2$, if the amplitude of the 5-pt function is large, $|h_{\text{NL}}^0| \gg |g_{\text{NL}}^0|$. However, we will not consider this last possibility in this work.

4. Implications on inflationary physics

The cumulation of long-wavelength fluctuations can generate significant variances in the small scale properties of primordial perturbations across the inflating space. If inflation lasted much longer than the $N_{\text{obs.}} \sim 60$ e-foldings corresponding to the horizon exit of the largest observable modes, this leads to a landscape picture where the properties of our observable patch depend on its location within the entire inflating space. This is qualitatively similar to the special case of the curvaton web discussed in [3].

The superhorizon variation is not measurable and the observable perturbations can be described by an effective model of inflation, covering only the last $N_{\text{obs.}}$ e-foldings. The effective model may however significantly differ from the fundamental model for the entire inflating epoch. The Lagrangian of the fundamental model is directly determined by the underlying high-energy physics which may also provide a natural range of initial conditions. In the effective model, the field values in the Lagrangian are shifted by random long-wavelength fluctuations. This may significantly affect the apparent form and predictions of the theory in the presence of isocurvature directions.

The ensemble averages calculable from the fundamental model correspond to the most likely predictions also in patches smaller than the inflating volume, at least in the perturbative regime we are considering here. The variances however make it possible to find substantial differences between the local and global properties of primordial perturbations. It is therefore of key interest to carefully explore the relation between the observable local quantities and the unobservable global inflationary perturbations which reflect the underlying high energy physics. In particular, the differences in non-Gaussian statistics over the entire inflating patch and our observable universe may easily become large with interesting consequences for observable quantities.

4.1 Small primordial non-Gaussianity

If Planck would not detect primordial non-Gaussianity, $|f_{\text{NL}}^{\text{obs}}| \lesssim 10$, then single-field slow-roll inflation would be favoured as the minimal scenario consistent with observations. However, nature might not have chosen the minimal setup. A small bispectrum $|f_{\text{NL}}^{\text{obs}}| \lesssim 10$ could also arise from models with significant non-Gaussianities in the form of trispectrum $|g_{\text{NL}}^{\text{obs.}}| \gg (f_{\text{NL}}^{\text{obs.}})^2$ (see [17, 18] for examples of such scenarios). The signal would remain unobserved by Planck if $|g_{\text{NL}}^{\text{obs.}}| \lesssim 10^4$ but could be revealed by future large scale surveys.

Using the landscape picture we introduced above, we can obtain novel insights on the naturalness of such models. The variance (3.6) of the locally observable bispectrum amplitude $f_{\text{NL}}^{\text{obs.}}$ grows as $\sigma_{f_{\text{NL}}} \propto g_{\text{NL}}^0 N_{\text{in.}}^{1/2}$ assuming that $(f_{\text{NL}}^0)^2 \ll g_{\text{NL}}^0$. Therefore, even if the global bispectrum would be small $|f_{\text{NL}}^0| < 10$, the probability for obtaining an unobservably small bispectrum amplitude $|f_{\text{NL}}^{\text{obs.}}| \lesssim 10$ in our patch decreases as g_{NL}^0 grows or

the inflationary epoch becomes longer. This is illustrated in the Fig. 2 which depicts the probability for $|f_{\text{NL}}^{\text{obs.}}| < 10$ as a function of f_{NL}^0 , g_{NL}^0 and $N_{\text{in.}}$, characterizing the fundamental inflationary model. For the parameter range shown in the figure, the variance of the spectrum is negligible compared to the observational accuracy $\sigma_{\mathcal{P}} \ll \Delta\mathcal{P}$ and we have thus set $\mathcal{P}_0 \simeq \mathcal{P}_{\text{obs.}} = 2.44 \times 10^{-9}$. The variance of trispectrum is also small so that $g_{\text{NL}}^{\text{obs.}} \simeq g_{\text{NL}}^0$ to a good precision.

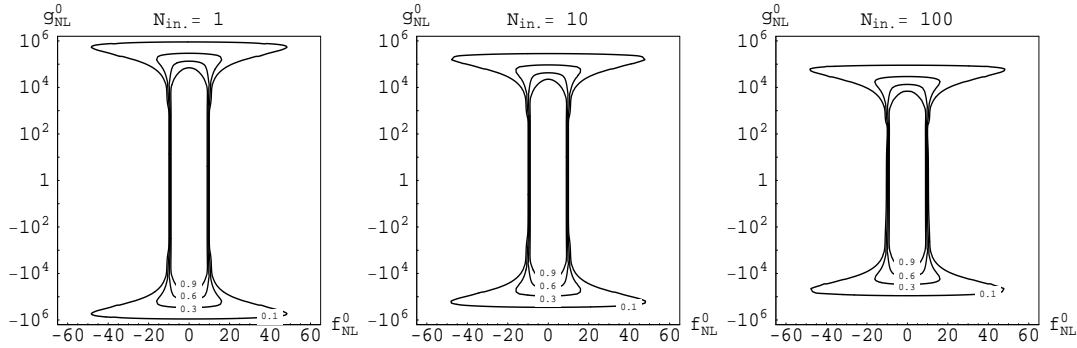


Figure 2: Probability to obtain a non-detectable bispectrum $|f_{\text{NL}}^{\text{obs.}}| < 10$ as a function of the ensemble expectation values f_{NL}^0 and g_{NL}^0 characterizing the underlying fundamental inflationary model. Three values of $N_{\text{in.}}$ are shown corresponding to different total durations of the inflationary epoch.

The figure shows that models with $|f_{\text{NL}}^0| \lesssim 10$ and $|g_{\text{NL}}^0| \lesssim 10^4$ have a high probability $P \gtrsim 0.9$ of producing unobservably small bispectrum $f_{\text{NL}}^{\text{obs.}}$ in our horizon patch. The probability is not sensitive to the duration of the inflationary epoch. We thus conclude (within the limits of validity of our perturbative treatment) that a small bispectrum $|f_{\text{NL}}^{\text{obs.}}| < 10$ is a natural outcome in inflationary models with a Lagrangian leading to $|f_{\text{NL}}^0| \lesssim 10$ and $|g_{\text{NL}}^0| \lesssim 10^4$.

On the other hand, Fig. 2 also shows that as the trispectrum grows observable $|g_{\text{NL}}^0| \simeq |g_{\text{NL}}^{\text{obs.}}| \gtrsim 10^4$ the probability for an unobservable bispectrum $|f_{\text{NL}}^{\text{obs.}}| < 10$ becomes smaller but not negligible. It is also interesting to note that an unobservable bispectrum can be generated even in models with a large global $|f_{\text{NL}}^0| \gtrsim 10$ even though the probability for this outcome is not higher than a few tens per cent at most. In the regime of large trispectrum $|g_{\text{NL}}^0| \gtrsim 10^4$ we also note that the probabilities become sensitively dependent on the amount of inflation $N_{\text{in.}}$ before our horizon exit. For example, the Fig. 2 shows that the probability to find $|f_{\text{NL}}^{\text{obs.}}| < 10$ and $|g_{\text{NL}}^{\text{obs.}}| \gtrsim 10^5$ becomes very small for $N_{\text{in.}} \gg 10$ while it may be substantially larger for $N_{\text{in.}} \lesssim 10$. Therefore, to generate a signature $|f_{\text{NL}}^{\text{obs.}}| \lesssim 10, |g_{\text{NL}}^{\text{obs.}}| \gtrsim 10^5$, inflation should not have lasted much longer than the observable $N_{\text{obs.}}$ e-foldings which represents a non-trivial tuning of model parameters.

We emphasize that our approach is model independent, apart from our restriction to the local form of non-Gaussianity (2.1). We therefore cannot address the possible fine-tuning associated to realizing specific values for f_{NL}^0 and g_{NL}^0 in a concrete inflationary setup. In contrast, our approach reveals that, independently of the details of inflationary

physics, certain configurations $f_{\text{NL}}^0, g_{\text{NL}}^0$ in general fail to translate into similar observational configurations $f_{\text{NL}}^{\text{obs}}, g_{\text{NL}}^{\text{obs}}$ unless non-trivial constraints are placed on the duration of inflationary epoch. We will address this model-independent tuning in more detail below.

4.2 Large primordial non-Gaussianity

In the regime of detectable bispectrum by Planck, $|f_{\text{NL}}^{\text{obs}}| \gtrsim 10$, the variance due to long wavelength modes can have interesting effects. As the variance grows bigger than the 1- σ accuracy of Planck, $\sigma_{f_{\text{NL}}} \gtrsim \Delta f_{\text{NL}} = 5$, the projection of observational constraints on to the model parameters f_{NL}^0 and g_{NL}^0 becomes non-trivial.

This is illustrated in Fig. 3. The figure depicts the relation between the observable $f_{\text{NL}}^{\text{obs}}$, and the theoretical parameters f_{NL}^0 and g_{NL}^0 directly connected to details of the underlying inflationary physics. The variance $\sigma_{f_{\text{NL}}}$ grows along with the number of e-foldings N_{in} .

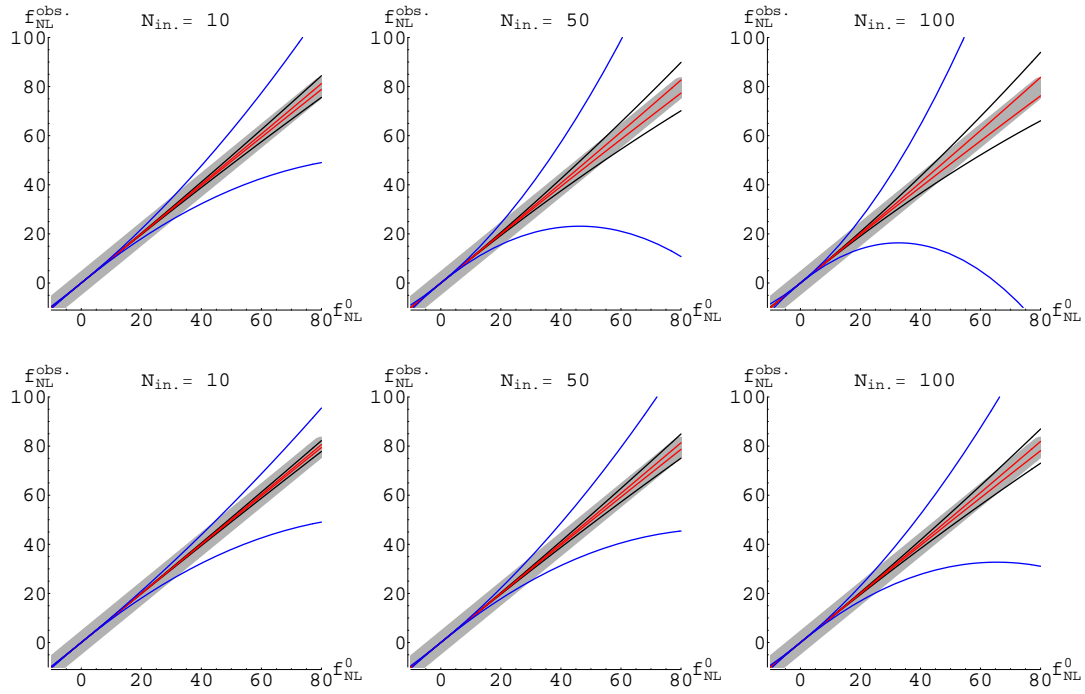


Figure 3: The observable bispectrum $f_{\text{NL}}^{\text{obs}}$ plotted against the theoretical expectation value f_{NL}^0 which reflects the underlying inflationary physics. The shaded area corresponds to the observational 1- σ uncertainty of Planck $\Delta f_{\text{NL}} = 5$. The curves in the upper panel bound the theoretical 2- σ regions $f_{\text{NL}}^{\text{obs}} = f_{\text{NL}}^0 \pm 2\sigma_{f_{\text{NL}}}$ of the bispectrum amplitude $f_{\text{NL}}^{\text{obs}}$ in our observable patch. The lower panel shows the corresponding 1- σ regions $f_{\text{NL}}^{\text{obs}} = f_{\text{NL}}^0 \pm \sigma_{f_{\text{NL}}}$. The three curves depict $g_{\text{NL}}^0 = 0$ (black, middle), $g_{\text{NL}}^0 = (f_{\text{NL}}^0)^2$ (red, innermost) and $g_{\text{NL}}^0 = 10(f_{\text{NL}}^0)^2$ (blue, outermost). The results are shown for three choices of N_{in} , the number of e-foldings before the horizon exit of largest observable scales. The variance of the spectrum is smaller than the observational error $\sigma_{\mathcal{P}}/\mathcal{P}_0 < 0.1$ in the entire regime shown in the plots.

preceding the horizon exit of largest observable modes. For $|g_{\text{NL}}^0| \gtrsim (f_{\text{NL}}^0)^2$, the 1- σ region of $f_{\text{NL}}^{\text{obs}}$ can grow so large that a detection of $f_{\text{NL}}^{\text{obs}}$ would not suffice to place tight constraints

on f_{NL}^0 . Consequently, the observable value $f_{\text{NL}}^{\text{obs.}}$ may considerably deviate from the global average f_{NL}^0 . The same would also be true for the trispectrum $g_{\text{NL}}^{\text{obs.}}$ if $|h_{\text{NL}}^0| \gg |g_{\text{NL}}^0|$, i.e. the 5-pt function would be large. Here we however do not consider this possibility further but restrict ourselves to models where $|h_{\text{NL}}^0| \lesssim |g_{\text{NL}}^0|$, and consequently $g_{\text{NL}}^{\text{obs.}} \simeq g_{\text{NL}}^0$.

We recap that f_{NL}^0 corresponds to the tree-level amplitude of the bispectrum computed for the inflationary model describing the evolution of the entire inflating patch. The form of this fundamental inflationary model is eventually dictated by the underlying high-energy physics and we denote its Lagrangian schematically by \mathcal{L}_0 . On the other hand, the properties of our observable patch can be parameterized by an effective model $\mathcal{L}_{\text{obs.}}$ describing only the last $N_{\text{obs.}} \sim 60$ e-foldings of inflation in our patch. Observables such as $f_{\text{NL}}^{\text{obs.}}$ then denote quantities calculable from the effective model $\mathcal{L}_{\text{obs.}}$. In the semiclassical approach that we are utilizing here, the field values of the effective Lagrangian are shifted by the random long-wavelength contributions, as is clear from equation (2.6). From the point of view of the effective model the shifts correspond to random changes of initial conditions if isocurvature directions are present during inflation. These can significantly affect the predictions, and especially the non-Gaussian statistics, generating substantial differences in the apparent form of the fundamental model \mathcal{L}_0 and the effective description of our patch $\mathcal{L}_{\text{obs.}}$. This has interesting ramifications as only the fundamental model \mathcal{L}_0 is the one directly reflecting the high energy physics behind the inflationary epoch whereas the effective model $\mathcal{L}_{\text{obs.}}$ is the one directly constrained by observations.

As the Fig. 3 illustrates, the variance $\sigma_{f_{\text{NL}}}$ can be large compared to the observational $1-\sigma$ error Δf_{NL} not only in models with $|g_{\text{NL}}^0| \gg (f_{\text{NL}}^0)^2$ but also for $|g_{\text{NL}}^0| \ll (f_{\text{NL}}^0)^2$ if f_{NL}^0 is large enough. As a curiosity, it is interesting to note that the variance is accidentally suppressed around $g_{\text{NL}}^0 \sim (f_{\text{NL}}^0)^2$ due to cancellation¹ of the two terms in (3.6). In this regime the predictions of the model are not significantly affected by the duration of inflation but the theoretical signature $g_{\text{NL}}^0 \sim (f_{\text{NL}}^0)^2$ is generically reflected with a high probability by the observables $g_{\text{NL}}^{\text{obs.}}$ and $f_{\text{NL}}^{\text{obs.}}$. This behaviour is illustrated in Fig. 4.

When the variance $\sigma_{f_{\text{NL}}}$ grows comparable to $|f_{\text{NL}}^0|$ the landscape effects become even more pronounced. In this regime the observational signature becomes dominated by the long-wavelength modes which may effectively screen the original signal f_{NL}^0 , reflecting the structure of the underlying inflationary physics. The locally measurable $f_{\text{NL}}^{\text{obs.}}$ then becomes strongly dependent on the location within the inflating patch and $f_{\text{NL}}^{\text{obs.}}$ may significantly deviate from the ensemble expectation value f_{NL}^0 . This behaviour can be observed in Fig. 5 which depicts the probability of generating an observable bispectrum as a function of the model parameters f_{NL}^0 and g_{NL}^0 . Indeed, in the regime $|g_{\text{NL}}^0| \gg (f_{\text{NL}}^0)^2$ where $\sigma_{f_{\text{NL}}}^2 \gg (f_{\text{NL}}^0)^2$ the probability for obtaining $10 < f_{\text{NL}}^{\text{obs.}} < 80$ remains non-negligible even for $f_{\text{NL}}^0 \gg 100$. The boundaries of the 60% probability contours in the f_{NL}^0 -direction however do not significantly differ from the bounds $10 < f_{\text{NL}}^{\text{obs.}} < 80$ unless the inflationary period becomes very long, $N_{\text{in}} \gtrsim 10^2$. The slow tightening of the upper bounds on f_{NL}^0 as a function of $N_{\text{in.}}$, as observed in the figure, is due to the growth of the variance $\sigma_{f_{\text{NL}}}$ (3.6). In the regime

¹The vanishing of $\sigma_{f_{\text{NL}}}$ for $g_{\text{NL}}^0 = 4/3(f_{\text{NL}}^0)^2$ (the proportionality factor depends on the Ansatz for the curvature perturbation, in our case eq. (2.1)) is an artefact of neglecting the slow roll corrections; in general they would generate a small $\sigma_{f_{\text{NL}}}$ even at $g_{\text{NL}}^0 = 4/3(f_{\text{NL}}^0)^2$.

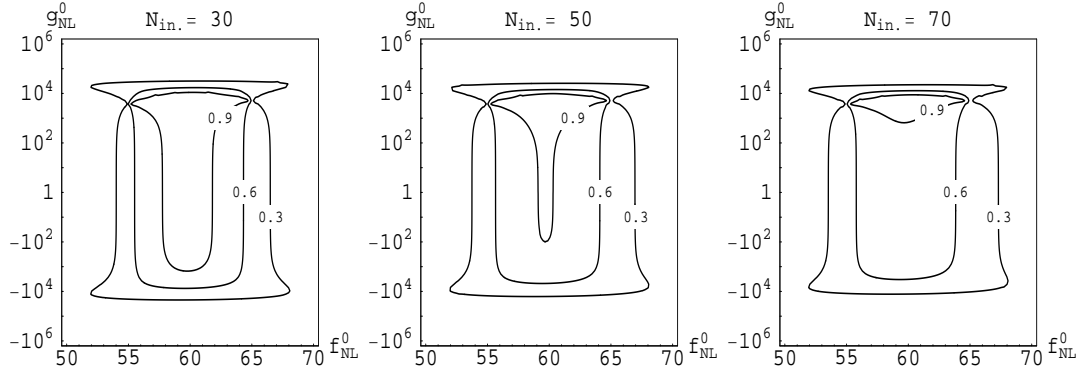


Figure 4: The contours depict the probability to obtain a bispectrum in the range $55 \leq f_{\text{NL}}^{\text{obs}} \leq 65$ as a function of the model parameters f_{NL}^0 and g_{NL}^0 . The results are shown for three choices of N_{in} , the number of e-foldings before the horizon exit of largest observable scales. The variance $\sigma_{f_{\text{NL}}}$ is accidentally suppressed for $g_{\text{NL}}^0 \sim (f_{\text{NL}}^0)^2$. This enhances the probability to produce large $f_{\text{NL}}^{\text{obs}}$ close to the ensemble average f_{NL}^0 of underlying inflationary physics.

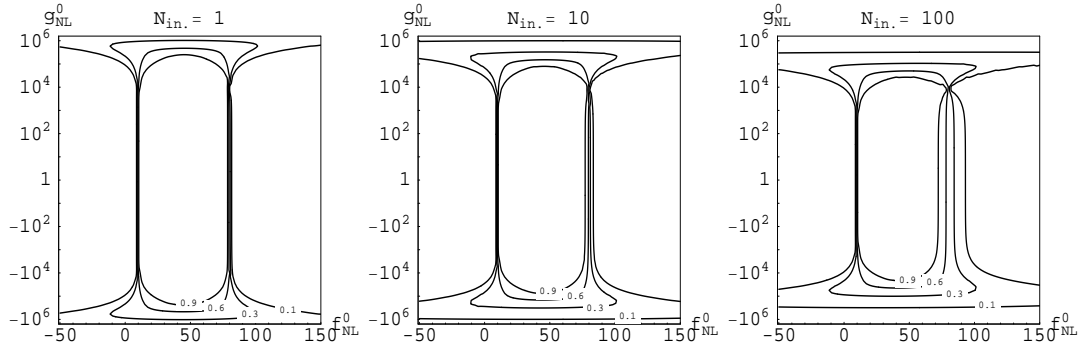


Figure 5: Probability to generate a bispectrum in the observable range $10 < |f_{\text{NL}}^{\text{obs}}| < 80$ as a function of the ensemble expectation values f_{NL}^0 and g_{NL}^0 . Three values of N_{in} are shown corresponding to different total durations of the inflationary epoch.

$g_{\text{NL}}^0 \sim (f_{\text{NL}}^0)^2$ the variance is suppressed which explains the different behaviour observed for these values in Fig. 5.

For even longer periods of inflation $N_{\text{in}} \gg 10^2$ the effects are expected to become even more significant. The analysis of this regime is however beyond the scope of the current work as our perturbative approach can not be directly applied to this regime without carefully addressing convergence issues.

4.3 Non-Gaussian signatures and fine-tuning

If the variances grow large, the observational configurations become sensitively dependent to N_{in} , the amount of inflation before our horizon exit. For the bispectrum this happens

when $|g_{\text{NL}}^0| \gg (f_{\text{NL}}^0)^2$ as can be clearly observed in Figs. 3 and 5.

Indeed, our findings show that observable patterns $\{f_{\text{NL}}^{\text{obs.}}, g_{\text{NL}}^{\text{obs.}}\}$ with $|g_{\text{NL}}^{\text{obs.}}| \gg (f_{\text{NL}}^{\text{obs.}})^2$ directly reflect the underlying theoretical signature $\{f_{\text{NL}}^0, g_{\text{NL}}^0\}$ only if that signature was realized just before the horizon exit of the observable scales. Consequently, as $\{f_{\text{NL}}^0, g_{\text{NL}}^0\}$ characterise correlators over the entire inflating space, this implies that inflation should not have lasted much longer than the observable $N_{\text{obs.}}$ e-foldings. If inflation lasted much longer, $N_{\text{in.}} \gg 1$, the rapidly growing variance of the bispectrum $\sigma_{f_{\text{NL}}}$ effectively screens the original signature $\{f_{\text{NL}}^0, g_{\text{NL}}^0\}$. The probability of $f_{\text{NL}}^{\text{obs.}}$ deviating from f_{NL}^0 then becomes significant and the observational configuration $\{f_{\text{NL}}^{\text{obs.}}, g_{\text{NL}}^{\text{obs.}}\}$ no longer reflects the theoretical signature $\{f_{\text{NL}}^0, g_{\text{NL}}^0\}$ dictated by the underlying inflationary physics. Related considerations were also made in [17].

There is no a priori reason why the inflationary epoch should not have lasted much longer than $N_{\text{obs.}}$ e-foldings, corresponding to the largest observable modes in the current universe. Consequently, requiring $N_{\text{in.}}$ to be small is a non-trivial constraint indicating generic tuning associated to configurations with large $g_{\text{NL}}^{\text{obs.}}$. The range of e-foldings $N_{\text{in.}}$ after which an original signature $|g_{\text{NL}}^0| \gg (f_{\text{NL}}^0)^2$ gets screened by the long-wavelength modes is depicted in Fig. 6 as a function of g_{NL}^0 . Note that since we assume the amplitude

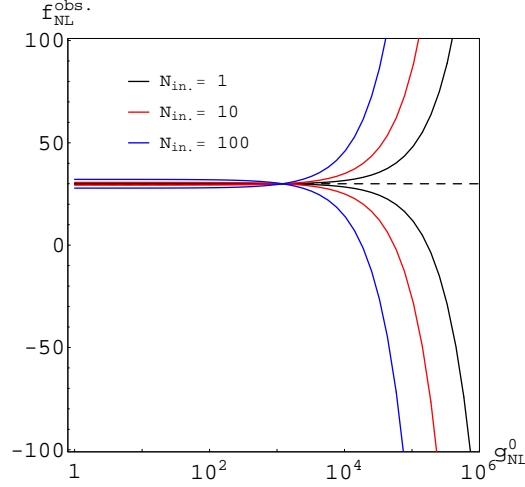


Figure 6: Configurations $|g_{\text{NL}}^0| \gg (f_{\text{NL}}^0)^2$ appear tuned as they become strongly modulated by long-wavelength modes if the horizon exit of the largest observable scales was preceded by even a few e-foldings of inflation. The dashed line depicts the value chosen for f_{NL}^0 , the amplitude of the bispectrum over the entire inflating patch which reflects the underlying inflationary physics.

of the 5-pt function is not exceptionally large, $|h_{\text{NL}}^0| \lesssim (f_{\text{NL}}^0)^3$, the variance of $g_{\text{NL}}^{\text{obs.}}$ is negligible, $\sigma_{g_{\text{NL}}}^2 \ll (g_{\text{NL}}^0)^2$, for the range of parameters we are considering. Therefore to a good precision we can approximate $g_{\text{NL}}^{\text{obs.}} \simeq g_{\text{NL}}^0$.

Fig. 6 shows that for signatures with $g_{\text{NL}}^{\text{obs.}} \sim 10^6$ and $(f_{\text{NL}}^{\text{obs.}})^2 \ll g_{\text{NL}}^{\text{obs.}}$, the bispectrum is dominated by the long-wavelength contributions already if $N_{\text{in.}} \gtrsim 1$. To translate a theoretical configuration $\{f_{\text{NL}}^0, g_{\text{NL}}^0\}$ with $|g_{\text{NL}}^0| \sim 10^6$ to the corresponding observational signature $\{f_{\text{NL}}^{\text{obs.}}, g_{\text{NL}}^{\text{obs.}}\}$, the parameters f_{NL}^0 and g_{NL}^0 should thus be tuned to the desired

values less than one e-folding before the horizon exit of the observable mode. If the values f_{NL}^0 and g_{NL}^0 are set at an earlier stage, the observable $f_{\text{NL}}^{\text{obs.}}$ has a high probability to significantly differ from the theoretical expectation f_{NL}^0 . This suggests that such configurations are not very natural – unless the model under consideration naturally generates $N_{\text{tot.}} \sim N_{\text{obs.}}$ e-foldings of inflation. For $|g_{\text{NL}}^{\text{obs.}}| \gtrsim 10^5$ the corresponding range of e-foldings is given by $N_{\text{in.}} \lesssim 10$ indicating a somewhat milder tuning. For $|g_{\text{NL}}^{\text{obs.}}| \gtrsim 10^4$ the constraint is relaxed to $N_{\text{in.}} \lesssim 100$.

We stress again that our discussion of the fine-tuning addresses only the probabilities of finding observational configurations $\{f_{\text{NL}}^{\text{obs.}}, g_{\text{NL}}^{\text{obs.}}\}$ in our horizon patch given that our horizon exit was preceded by some e-foldings of inflation. The naturalness of realising certain values of $f_{\text{NL}}^0, g_{\text{NL}}^0$ in specific inflationary models is another, model dependent issue which may give rise to further tuning, or favour specific signatures. Our general approach instead addresses the way how the theoretical configurations f_{NL}^0 and g_{NL}^0 translate into measurable properties in our observable patch. As we have shown, for the class of models with $|g_{\text{NL}}^0| \gg (f_{\text{NL}}^0)^2$ these considerations suggest that converting the value f_{NL}^0 into the corresponding observational value $f_{\text{NL}}^{\text{obs.}} \sim f_{\text{NL}}^0$ becomes unlikely unless the horizon exit of our observable patch occurs soon after the beginning of inflation. Imposing this requirement indicates a generic source of non-trivial tuning in models with $|g_{\text{NL}}^0| \gg (f_{\text{NL}}^0)^2$.

5. Extension and applications of our results

5.1 Variance of the power spectrum in multi-source scenarios

In this paper we have focused on single-source scenarios, and shown under which circumstances there may be a significant variance of observable quantities when making observations in a patch smaller than the total inflated volume. Redoing this analysis in multi-source scenarios goes beyond the scope of this work, but our formalism makes it possible to do so, and here we give one small example, thereby showing that our considerations remain interesting in multi-source cases.

In a multi-source scenario, we must take into account the effect of all relevant long wavelength fluctuations on to the short wavelength modes. For the power spectrum, the lowest order correction comes from the influence of the linear long wavelength modes on to the linear short wavelength modes

$$\zeta_{\text{obs.}} = N_A^0 \delta\sigma_s^A + N_{AB}^0 \delta\sigma_s^A \delta\sigma_L^B + \dots, \quad (5.1)$$

where summation convention is used for the field indices, A, B, \dots , over all field components.

At tree level, and assuming that each component of the field perturbations are uncorrelated, we may use

$$\mathcal{P}_0 = N_A^0 N^{0,A} \mathcal{P}_\sigma, \quad \frac{6}{5} f_{\text{NL}}^0 = \frac{N_{AB}^0 N^{0,A} N^{0,B}}{(N_C^0 N^{0,C})^2}, \quad \tau_{\text{NL}}^0 = \frac{N_A^0 N_B^{0,A} N_C^B N^C}{(N_D^0 N^{0,D})^2}. \quad (5.2)$$

Hence

$$\langle \zeta_{\text{obs.}, \mathbf{k}_1} \zeta_{\text{obs.}, \mathbf{k}_2} \rangle = N_A^0 N_B^0 \langle \delta\sigma_{\mathbf{s}, \mathbf{k}_1}^A \delta\sigma_{\mathbf{s}, \mathbf{k}_2}^B \rangle + (N_A^0 N_{BC}^0 \langle \delta\sigma_{\mathbf{s}, \mathbf{k}_1}^A \delta\sigma_{\mathbf{s}, \mathbf{k}_2}^B \rangle \delta\sigma_L^C + 1 \text{ perm.}) \quad (5.3)$$

$$\mathcal{P}_{\text{obs.}} = \mathcal{P}_0 \left(1 + 2 \frac{N_A^0 N_B^0 \delta\sigma_L^B}{N_C^0 N_{0,C}} \right), \quad (5.4)$$

$$\sigma_{\mathcal{P}}^{2, \text{multi}} = 4\tau_{\text{NL}}^0 \mathcal{P}_0^3 N_{\text{in.}}. \quad (5.5)$$

Applying the Suyama-Yamaguchi (SY) inequality $\tau_{\text{NL}}^0 \geq (6f_{\text{NL}}^0/5)^2$ [19], it follows that

$$\sigma_{\mathcal{P}}^{2, \text{multi}} \geq \left(\frac{12}{5} f_{\text{NL}}^0 \right)^2 \mathcal{P}_0^3 N_{\text{in.}} = \sigma_{\mathcal{P}}^{2, \text{single}}. \quad (5.6)$$

Hence for a given value of f_{NL}^0 , the variance of the power spectrum is larger than in single-source scenarios, showing that our consideration about the difference between observables in the entire inflated patch and our observable patch may become even more important in multi-source scenarios.

5.2 What will we observe if the single-source equality is broken by loops?

Since we have assumed in most of this paper that we are in a single-source scenario, it is interesting to consider how we can observationally check whether this is the case. The well known test is the equality $\tau_{\text{NL}}^{\text{obs.}} = (6f_{\text{NL}}^{\text{obs.}}/5)^2$ which however is only valid at tree-level [2, 20]. In what follows we are mainly considering quantities in our observable patch and for brevity we omit the labels ^{obs.} where no risk for confusion arises and simply denote $f_{\text{NL}} \equiv f_{\text{NL}}^{\text{obs.}}$ etc. Loop effects can most easily break the equality when g_{NL} is large, a scenario we have extensively studied in this paper, making this particularly relevant to study here. This would cause a deviation from the equality when considering loop corrected quantities at scales smaller than our horizon patch. However there is a generalised equality between radiatively corrected quantities which include both loop corrections where internal momenta are integrated over and soft corrections where external momenta become small. This new equality is valid to all orders in radiative corrections and it provides a new test of inflation, as shown in [15].

A priori, in order to see a breaking of the equality, τ_{NL} is the only parameter which we need to observe, regardless of whether it is broken by loops in a single-source scenario, or by multi-source effects. Here we will show that in practice if it is broken by loops, we are essentially guaranteed to see all three non-linearity parameters. The calculation is restricted to the one loop level.

To be concrete, we assume that Planck can detect non-linearity parameters with $2 - \sigma$ confidence if $f_{\text{NL}} > 10$, $\tau_{\text{NL}} > 10^3$, $g_{\text{NL}} > 10^4$ [21, 22].

Assuming that the SY inequality is always valid [23, 20, 24, 25], to see a breaking of the equality with Planck we have to observe $10^3 \lesssim \tau_{\text{NL}} \lesssim 10^4$ where the upper bound comes from the current observational constraint. In this case $30 \lesssim |f_{\text{NL}}| \lesssim 10^2$ if the equality holds and we would clearly observe f_{NL} as well. The key observation is that in order for f_{NL} not to be seen, $|f_{\text{NL}}| \lesssim 10$, we need $A_{\text{NL}} \equiv \tau_{\text{NL}}/(6f_{\text{NL}}/5)^2 \gtrsim 10^3/10^2 \sim 10$, so the

equality needs to be strongly broken in this case. From [15] we find at one-loop level

$$A_{\text{NL}} \equiv \left(\frac{5}{6}\right)^2 \left(\frac{\tau_{\text{NL}}}{f_{\text{NL}}^2}\right)_{\text{tree+loop}} \simeq 1 + 4 \left(\frac{g_{\text{NL}}}{f_{\text{NL}}}\right)_{\text{tree}}^2 \mathcal{P}, \quad (5.7)$$

where the second term on the right hand side of the last equality is responsible for breaking the equality. In order to get $A_{\text{NL}} \gtrsim 10$ with $|f_{\text{NL}}| \lesssim 10$ we should then have $|g_{\text{NL}}| \gtrsim 3 \times 10^5 \gg f_{\text{NL}}^2$ at tree-level and hence the “normal” hierarchy between g_{NL} and f_{NL} must also be strongly broken. A breaking of the equality must therefore come through an observably large g_{NL} , which is close to the current upper limit. Such a large tree-level g_{NL} does not create problems with a loop correction to either f_{NL} or the power spectrum, and the perturbative expansion in loops remains valid [15].

Finally given that we require such a large value of $g_{\text{NL}}^{\text{obs.}}$, what is the probability that $f_{\text{NL}}^{\text{obs.}}$ is too small to be seen in our Hubble volume value? The answer can be seen in Fig. 2, for $|g_{\text{NL}}^{\text{obs.}}| \simeq |g_{\text{NL}}^0| \gtrsim 10^5$ the probability of obtaining $|f_{\text{NL}}^{\text{obs.}}| < 10$ is suppressed below about 50% already for $N_{\text{in.}} \sim 1$ and it rapidly decreases as $N_{\text{in.}}$ grows. We may thus conclude that a breaking of the SY equality in single-source inflation is likely to be accompanied by a measurement of all three non-linearity parameters. It should then also be possible to observe our equality $\tau_{\text{NL}}^{\text{rad.}} = (6/5)^2 (f_{\text{NL}}^{\text{rad.}})^2$ between the radiatively corrected quantities $\tau_{\text{NL}}^{\text{rad.}}$ and $f_{\text{NL}}^{\text{rad.}}$ which contain not only the loop corrections but also the corrections from soft modes [2, 15].

6. Conclusions

Primordial perturbations with wavelengths greater than the observable universe contribute to background quantities in our observable patch. The long-wavelength contributions vary across the inflating patch and amount to random shifts of the local field expectation values. This leads to a landscape picture where the properties of our observable patch depend on its location. The observable primordial perturbations constrain the form of the effective model for the last $N_{\text{obs.}}$ e-foldings of inflation in our observable patch. Being affected by random long-wavelength contributions the effective model may considerably differ from the fundamental model of inflation which describes the entire inflating patch and whose form is dictated by the underlying high energy physics.

In this work we have shown that if multiple fields are present during inflation, the long-wavelength contributions can be significant even if our horizon exit would be preceded by only a few e-foldings of inflation. Long-wavelength modes generate shifts along isocurvature directions which correspond to non-trivial changes of initial conditions in the effective model and can greatly affect the resulting perturbations, especially the non-Gaussian statistics. In particular, the impact of the long-wavelength modes can not be deduced from the effective model itself but they reflect the form of the underlying fundamental model of inflation. This is in sharp contrast to pure single field slow roll models where the long-wavelength effects are slow roll suppressed and amount to local time shifts expressible in terms of spectral indices. As the simplest example of multiple field models, we have in this work concentrated on long-wavelength effects in the generic class of single source models with the local type

of non-Gaussianity. Many theoretically interesting models, for example the curvaton and modulated reheating scenarios in the limit of negligible inflaton perturbations, fall into this class of models where perturbations are generated by a single inhomogeneous field, despite the presence of several light fields during inflation.

We have found novel general relations between the primordial perturbations in our observable part of the universe and the inflationary physics controlling the entire inflating patch. We have investigated the consequences of both a detection and non-detection of the primordial bispectrum $f_{\text{NL}}^{\text{obs.}}$ by Planck. Our results demonstrate that an eventual non-detection would not strictly rule out models with a large bispectrum. Indeed if inflation lasted longer than the observable $N_{\text{obs.}}$ e-foldings, models with a bispectrum up to $f_{\text{NL}}^0 \sim 40$ when averaged over the entire inflating patch, can have a probability up to few tens of per cents for yielding $|f_{\text{NL}}^{\text{obs.}}| \lesssim 10$ in our observable patch. However, this is not a very generic feature but requires a large trispectrum amplitude $|g_{\text{NL}}^0| \gtrsim 10^4$ and a value of g_{NL}^0 falling to a specific narrow range.

In case f_{NL} is detected, the long-wavelength effects quite generically have interesting implications for the interpretation of the observation. If the inflationary model predicts $g_{\text{NL}}^0 \gtrsim (f_{\text{NL}}^0)^2$ across the entire inflating patch, we find that the observable bispectrum $f_{\text{NL}}^{\text{obs.}}$ has a high probability to deviate from the global mean f_{NL}^0 even if there were only a few tens of e-foldings of inflation before our horizon exit. As we have shown in this work, the observational constraints on $f_{\text{NL}}^{\text{obs.}}$ therefore translate in a highly non-trivial way on the parameters f_{NL}^0 , g_{NL}^0 , characterizing the underlying inflationary physics.

We have also shown that inflationary models predicting a hierarchy $|g_{\text{NL}}^0| \gg (f_{\text{NL}}^0)^2$ imply an inherent tuning of the total duration of inflation irrespective of details of the inflationary physics. This is because the variance of the bispectrum easily becomes very large after a short period of inflation making it unlikely to find an observable value $f_{\text{NL}}^{\text{obs.}}$ which would reflect the global mean f_{NL}^0 . For $|g_{\text{NL}}^0| \sim 10^6$ this happens if our horizon exit was preceded by just one e-folding of inflation and for $|g_{\text{NL}}^0| \sim 10^5$ after about ten e-foldings. To translate a theoretical configuration $|g_{\text{NL}}^0| \gg (f_{\text{NL}}^0)^2$ to the corresponding observational signature, the total duration of inflationary epoch should not be much longer than the observable e-foldings $N_{\text{obs.}}$. This tuning represents a highly non-trivial constraint on inflationary physics.

It would be interesting to extend our results to generic multiple field models where the long-wavelength effects could be even more pronounced, as we have briefly discussed above. Another interesting line of future work would be to consider non-Gaussianities generated by subhorizon physics which generate non-trivial deviations from the local form. Developing a solid understanding of the long-wavelength effects would indeed be of key importance as it appears to play an essential role in translating the new observational data into a deeper understanding of fundamental high-energy physics.

Note added Whilst this paper was being completed, a related work appeared on the arxiv by Nelson and Shandera [26]. This work is conceptually similar to ours, since it also studies the relation between our observable correlators to those in a much larger patch in single-source scenarios and focusing on the local model. However their focus is on the

structure and hierarchy of the non-Gaussian moments, while we focused on more concrete calculations, such as explicitly finding how much f_{NL} varies under the influence of g_{NL} . This paper and [26] are therefore complementary.

Acknowledgments

We thank Jussi Väliiviita and Matti Savelainen for helpful discussions on statistics. S.N. is supported by the Academy of Finland grant 257532. C.B. is supported by a Royal Society University Research Fellowship. G.T. is supported by an STFC Advanced Fellowship ST/H005498/1. C.B. and G.T. would like to thank the theory group of Nordita, Stockholm for their warm hospitality.

References

- [1] S. B. Giddings, M. S. Sloth, JCAP **1101** (2011) 023. [arXiv:1005.1056 [hep-th]]; M. Gerstenlauer, A. Hebecker, G. Tasinato, JCAP **1106** (2011) 021. [arXiv:1102.0560 [astro-ph.CO]]; C. T. Byrnes, M. Gerstenlauer, A. Hebecker, S. Nurmi, G. Tasinato, JCAP **1008** (2010) 006. [arXiv:1005.3307 [hep-th]]; Y. Urakawa, T. Tanaka, Phys. Rev. **D82** (2010) 121301. [arXiv:1007.0468 [hep-th]]; W. Unruh, “Cosmological long wavelength perturbations,” [astro-ph/9802323]; Y. Urakawa, Prog. Theor. Phys. **126** (2011) 961 [arXiv:1105.1078 [hep-th]]; S. B. Giddings, M. S. Sloth, Phys. Rev. D **86** (2012) 083538 [arXiv:1109.1000 [hep-th]]; L. Senatore and M. Zaldarriaga, “On Loops in Inflation II: IR Effects in Single Clock Inflation,” arXiv:1203.6354 [hep-th].
- [2] C. T. Byrnes, S. Nurmi, G. Tasinato and D. Wands, JCAP **1203**, 012 (2012) [arXiv:1111.2721 [astro-ph.CO]].
- [3] A. D. Linde and V. Mukhanov, JCAP **0604** (2006) 009 [astro-ph/0511736].
- [4] V. Demozzi, A. Linde and V. Mukhanov, JCAP **1104**, 013 (2011) [arXiv:1012.0549 [hep-th]].
- [5] T. Suyama, T. Takahashi, M. Yamaguchi and S. Yokoyama, JCAP **1012**, 030 (2010) [arXiv:1009.1979 [astro-ph.CO]].
- [6] K. Enqvist and M. S. Sloth, Nucl. Phys. B **626**, 395 (2002) [arXiv:hep-ph/0109214]; D. H. Lyth and D. Wands, Phys. Lett. B **524**, 5 (2002) [arXiv:hep-ph/0110002]; T. Moroi and T. Takahashi, Phys. Lett. B **522**, 215 (2001) [Erratum-ibid. B **539**, 303 (2002)] [arXiv:hep-ph/0110096]; A. D. Linde and V. F. Mukhanov, Phys. Rev. D **56** (1997) 535 [arXiv:astro-ph/9610219]; S. Mollerach, Phys. Rev. D **42** (1990) 313.
- [7] D. H. Lyth, C. Ungarelli and D. Wands, Phys. Rev. D **67**, 023503 (2003) [arXiv:astro-ph/0208055].
- [8] G. Dvali, A. Gruzinov and M. Zaldarriaga, Phys. Rev. D **69**, 023505 (2004) [arXiv:astro-ph/0303591].
- [9] L. Kofman, “Probing string theory with modulated cosmological fluctuations,” arXiv:astro-ph/0303614.
- [10] C. T. Byrnes, M. Gerstenlauer, S. Nurmi, G. Tasinato, D. Wands, JCAP **1010**, 004 (2010). [arXiv:1007.4277 [astro-ph.CO]]; C. T. Byrnes, S. Nurmi, G. Tasinato, D. Wands, JCAP **1002** (2010) 034. [arXiv:0911.2780 [astro-ph.CO]].

- [11] A. A. Starobinsky, JETP Lett. **42**, 152 (1985) [Pisma Zh. Eksp. Teor. Fiz. **42**, 124 (1985)];
M. Sasaki and E. D. Stewart, Prog. Theor. Phys. **95** (1996) 71 [arXiv:astro-ph/9507001];
M. Sasaki and T. Tanaka, Prog. Theor. Phys. **99**, 763 (1998) [arXiv:gr-qc/9801017].
- [12] T. Okamoto and W. Hu, Phys. Rev. D **66** (2002) 063008 [astro-ph/0206155].
- [13] C. T. Byrnes, M. Sasaki and D. Wands, Phys. Rev. D **74**, 123519 (2006) [astro-ph/0611075].
- [14] D. H. Lyth, JCAP **0712** (2007) 016 [arXiv:0707.0361 [astro-ph]].
- [15] G. Tasinato, C. T. Byrnes, S. Nurmi and D. Wands, arXiv:1207.1772 [hep-th].
- [16] E. Komatsu and D. N. Spergel, Phys. Rev. D **63** (2001) 063002 [astro-ph/0005036];
M. Liguori and A. Riotto, Phys. Rev. D **78** (2008) 123004 [arXiv:0808.3255 [astro-ph]].
- [17] F. Bernardeau and J. -P. Uzan, Phys. Rev. D **70**, 043533 (2004) [astro-ph/0311421].
- [18] K. Enqvist and T. Takahashi, JCAP **0809** (2008) 012 [arXiv:0807.3069 [astro-ph]];
K. Enqvist, S. Nurmi, O. Taanila and T. Takahashi, JCAP **1004** (2010) 009 [arXiv:0912.4657
[astro-ph.CO]]; K. Enqvist and S. Nurmi, JCAP **0510** (2005) 013 [astro-ph/0508573];
Q. -G. Huang, JCAP **0811** (2008) 005 [arXiv:0808.1793 [hep-th]]; C. T. Byrnes and
G. Tasinato, JCAP **0908** (2009) 016 [arXiv:0906.0767 [astro-ph.CO]].
- [19] T. Suyama and M. Yamaguchi, Phys. Rev. D **77**, 023505 (2008) [arXiv:0709.2545 [astro-ph]].
- [20] N. S. Sugiyama, JCAP **1205**, 032 (2012) [arXiv:1201.4048 [gr-qc]].
- [21] N. Kogo and E. Komatsu, Phys. Rev. D **73**, 083007 (2006) [astro-ph/0602099].
- [22] J. Smidt, A. Amblard, C. T. Byrnes, A. Cooray, A. Heavens and D. Munshi, Phys. Rev. D
81, 123007 (2010) [arXiv:1004.1409 [astro-ph.CO]].
- [23] K. M. Smith, M. LoVerde and M. Zaldarriaga, Phys. Rev. Lett. **107**, 191301 (2011)
[arXiv:1108.1805 [astro-ph.CO]].
- [24] V. Assassi, D. Baumann and D. Green, JCAP **1211**, 047 (2012) [arXiv:1204.4207 [hep-th]].
- [25] A. Kehagias and A. Riotto, Nucl. Phys. B **864**, 492 (2012) [arXiv:1205.1523 [hep-th]].
- [26] E. Nelson and S. Shandera, arXiv:1212.4550 [astro-ph.CO].